The Planetary Science Journal, 6:32 (10pp), 2025 February https://doi.org/10.3847/PSJ/ad9d3f

Ariel's Medial Grooves: Spreading Centers on a Candidate Ocean World

Chloe B. Beddingfield, Richard J. Cartwright, Lauren M. Jozwiak, Tom A. Nordheim, and G. Wes Patterson
Johns Hopkins University Applied Physics Laboratory, Laurel, MD 20723, USA; chloe.beddingfield@jhuapl.gov
Received 2024 September 25; revised 2024 December 9; accepted 2024 December 9; published 2025 February 3

Abstract

We present evidence that Ariel's massive chasma-medial groove systems formed via spreading, where internally sourced material ascended and formed new crust. Evidence for this interpretation includes close alignment of offset faults and chasma margins during reconstruction, axial troughs bounded by raised rims, bowed-up chasma floors with marginal valleys, subparallel chasma floor ridges, and relatively young medial groove–bounding terrain. Ariel's medial grooves are among the youngest known Uranian moon geologic features and might be conduits to the interior and the source of NH-bearing species, CO, CO_2, and other potential internally derived volatiles detected on the surface. While medial grooves are observable in Brownie and Kewpie Chasmata, our results indicate that these features are also present below Voyager 2 Imaging Science System image resolutions in Korrigan, Pixie, and Sylph Chasmata. Close flybys of Ariel with a Uranus orbiter are imperative to uncover the nature of these curious features and to gain insight into this moon's most recent geologic events.

Unified Astronomy Thesaurus concepts: Uranian satellites (1750); Tectonics (2175); Planetary science (1255); Natural satellite surfaces (2208); Natural satellites (Solar system) (1089)

1. Introduction

Ariel is a candidate ocean world, and recent observations from the James Webb Space Telescope (JWST) confirmed that its surface is mantled by a large amount of CO_2 ice mixed with lower amounts of CO ice (R. J. Cartwright et al. 2024). These species are unstable at Ariel's estimated peak surface temperatures (80–90 K; R. Hanel et al. 1986; M. M. Sori et al. 2017) and should sublimate and gradually escape to space (e.g., M. M. Sori et al. 2017; S. M. Menten et al. 2024). Consequently, the observed constituents on Ariel are likely replenished, possibly from endogenic sources (R. J. Cartwright et al. 2024). Additionally, ground-based telescope observations have identified spectral evidence for ammonia (NH)-bearing species, which may also be sourced from Ariel's interior (R. J. Cartwright et al. 2020). The geologic conduits utilized by these volatiles to reach Ariel's surface, however, have not been identified.

Ariel's "medial grooves," present within the massive chasmata (Figure 1), cut across the relatively young chasma floors (although their absolute ages are unknown) and therefore likely represent the youngest features identified on Ariel's surface. These medial grooves are reminiscent of geologic features on Earth associated with volcanic activity such as fissures (S. Croft & L. Soderblom 1991), erupted lava tubes (D. Rothery 1990), and spreading centers (J. Kargel 1988). All three of these candidate analogs are consistent with possible conduits between Ariel's interior and exterior, potentially capable of delivering volatile components to the surface. In this work, we investigate the formation mechanisms for Ariel's medial grooves and present evidence that they are most consistent with spreading centers.

2. Ariel's Geology

Geologic Units and Surface Features. The portion of Ariel's surface imaged by the Imaging Science System (ISS) on board Voyager 2 has been separated into four broad geologic units (S. Croft & L. Soderblom 1991): the Cratered Plains that represent Ariel's oldest known terrain (1.3–0.6/+2.0 Ga, M. R. Kirchoff et al. 2022) and three younger units that are subdivided based on their relative ages (B. A. Smith et al. 1986; D. G. Jankowski & S. W. Squyres 1988). These younger units include the Older, Intermediate, and Young Smooth Materials units (Figure 1). These smooth materials units make up the floors of Ariel's massive and widespread canyons termed "chasmata" (B. A. Smith et al. 1986; J. Plescia 1987; S. Croft & L. Soderblom 1991); however, absolute modeled ages for the chasma floors are not available. The chasma boundaries are defined by large normal fault scarps, which are hundreds of kilometers in length and up to 4 km in height in some locations (P. Thomas 1988; P. M. Schenk & J. M. Moore 2020; C. B. Beddingfield et al. 2022).

The floors of Ariel's Pixie Group of chasmata fall into the "Intermediate Age Smooth Materials" unit (orange unit in Figure 1). The Pixie Group includes the following chasmata: Pixie, Brownie, Kewpie, Korrigan, Kra, and Sylph. The Kachina Group includes all chasmata within Kachina Chasmata. While the portion of Ariel's Cratered Plains cut by Kachina Chasmata faults and fractures is estimated to be 0.8 (−0.5/+1.8) Ga (M. R. Kirchoff et al. 2022), absolute modeled ages for the smooth materials units that make up the chasma floors have not been estimated (see Figure 2 in M. R. Kirchoff et al. 2022). The chasma floors are interpreted to be young based on the apparent low density of impact craters on this terrain relative to the adjacent Cratered Plains. The Pixie Group of chasmata are centered on Ariel's Uranus-facing hemisphere (0°), between 290° and 40° longitude. Much of the area containing these chasmata are north of −45° and extend beyond the equatorial region and terminator in ISS images. Based on the large chasma widths along the terminator, these

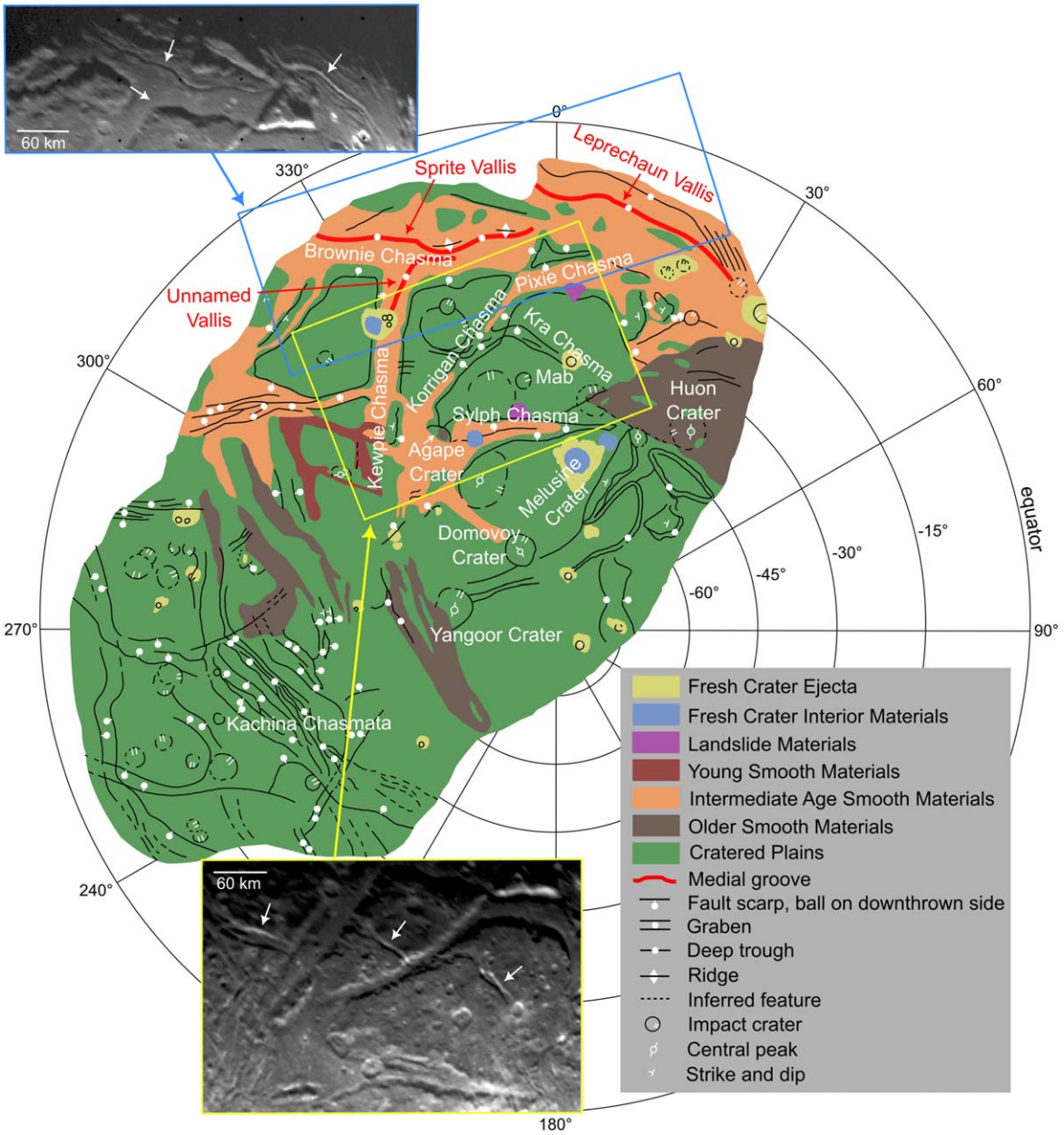

Figure 1. Geologic map and Voyager 2 ISS images of Ariel. The base figure is a digitized and modified version of the geologic map presented in S. Croft & L. Soderblom (1991). Locations of the three known medial grooves are shown in red. See S. Croft & L. Soderblom (1991) for detailed descriptions of mapped units and geologic features. The top blue-bordered Voyager 2 ISS image covers the three medial grooves identified on Ariel (arrows) and where they disappear beyond the terminator (c2684539, V. I. S. Team 1988, 995 m pixel^{-1}). The bottom yellow-bordered ISS image covers three offset fracture systems including Kra Chasma (arrows; c2684535, V. I. S. Team 1988, 999 m pixel^{-1}). While CO and CO_2 exhibit stronger spectral features over Ariel's trialing hemisphere, observations by JWST and ground-based facilities are disk integrated, and we cannot discern finer detail on the distribution of these constituents, even at the regional scale. Understanding the spatial relationship between geologic features like medial grooves and carbon oxides is not possible at this time and requires high spatial resolution spectral data collected during close flybys by a Uranus orbiter.

features likely extend well past the equator into northern latitudes.

Medial grooves are observable on the floors of two of Ariel's large chasmata (Figure 1) and are bounded by elevated ridges in some areas (Profile A–A′ in Figure 2(b)). Brownie Chasma contains Sprite Vallis and Leprechaun Vallis. Kewpie Chasma contains an unnamed medial groove, which we refer to as "Unnamed Vallis." Unnamed Vallis was mapped by S. Croft & L. Soderblom (1991) based on the interpretation of shadowing in Voyager 2 images, which revealed two adjacent ridges in this location, like the other more prominent medial grooves. While not provided a name in Ariel's most recent geologic map (S. Croft & L. Soderblom 1991), Unnamed Vallis was mapped as a "deep trough," like the other two medial grooves. Leprechaun, Sprite, and Unnamed Vallis are each greater than 300 km in length. However, Unnamed Vallis is notably thinner than Sprite or Leprechaun. While Sprite and Leprechaun Valles are up to a few tens of kilometers in width in some locations, the width of Unnamed Vallis is similar to the highest resolution of the available Voyager 2 ISS image of this area (c2684539, V. I. S. Team 1988, 995 m pixel^{-1}) and is only mapped in the northernmost section of Kewpie Chasma. Therefore, additional portions of Unnamed Vallis are likely present but too thin to be observed in available ISS images. Additional smaller medial

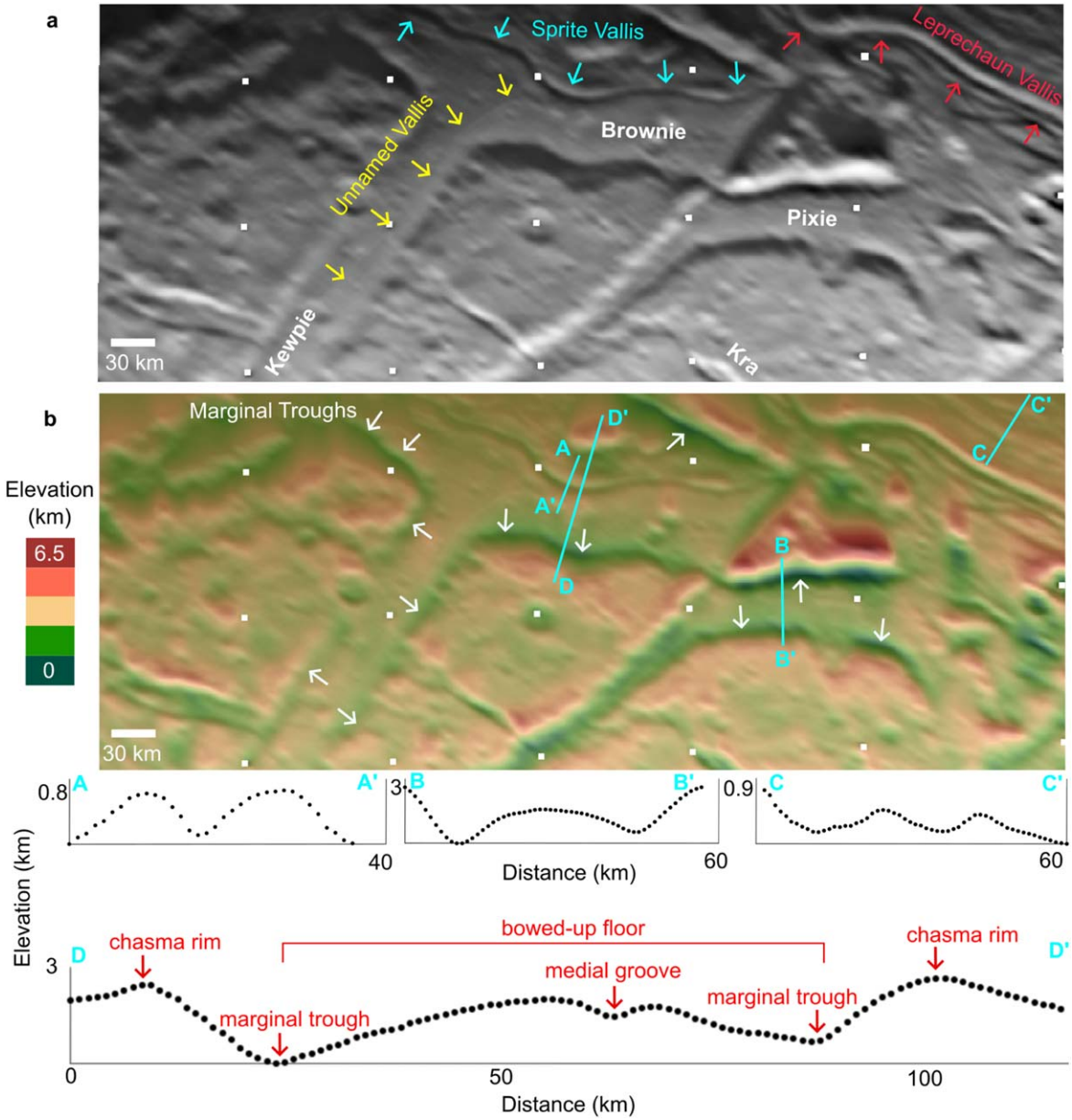

Figure 2. (a) Orthorectified Voyager 2 ISS image c2684539 (V. I. S. Team 1988, 995 m pixel^{-1}) showing the locations of Ariel's three identified medial grooves, Unnamed, Sprite, and Leprechaun Valles. The chasmata in this area are labeled in white. See Figure 1 for latitude and longitude information for these features. (b) A digital elevation model (DEM) showing the topography of the region covered in panel (a). White arrows show locations of the marginal valleys. See Sections 2.1 and A.1 in C. B. Beddingfield et al. (2022) for discussion on how this DEM was generated. The spatial resolution of the DEM is 995 m pixel^{-1}. White dots are associated with reseau points in panels (a) and (b). Topographic profiles show the following: A–A′: axial troughs with raised rims making up the medial groove called Sprite Vallis. B–B′: the bowed-up chasma floor and bounding marginal valleys of Pixie Chasma. C–C′: subparallel ridges bounding the medial groove called Leprechaun Vallis. D–D′: a full profile across the chasma-medial groove system of Brownie Chasma and Sprite Vallis.

grooves may be present, but their detection could be hindered by the low resolution of the available Voyager 2 ISS images covering Ariel's surface. Where observable, medial grooves run subparallel to adjacent chasma walls (Figure 1). Leprechaun Vallis, Sprite Vallis, and the adjacent walls of Brownie Chasma trend east–west, and Unnamed Vallis and both walls of Kewpie Chasma trend northeast–southwest. The margins of the chasma floors, at the base of the bounding normal fault scarps, are topographic lows (white arrows and Profile B–B′ in Figure 2(b)) relative to the bowed-up centers of the chasma floors.

Relative age estimates of Ariel's two chasma systems (the "Pixie Group" and the "Kachina Group") are based on the degradation states of chasma rims and the number of overprinting impact craters on these rims (S. Croft & L. Soderblom 1991). These analyses indicate that Kachina Chasmata exhibits sharper rims that appear to have undergone less degradation and therefore is likely younger than the chasmata that make up the Pixie Group. The older Pixie Group includes the following chasmata: Pixie, Kewpie, Brownie, Kra, Sylph, and an unnamed chasma. The younger Kachina Group is made up only of the faults comprising Kachina Chasmata. However, it is unknown what the absolute difference in age is between the Kachina Group and the Pixie Group.

Surface Composition. Observations of Ariel made by ground-based telescopes have detected weak spectral features between

2.12 and 2.27 μm that may result from NH-bearing species (R. J. Cartwright et al. 2018, 2020). NH-rich materials were likely incorporated into Ariel and the other Uranian moons as they formed in Uranus's subnebula (e.g., J. S. Lewis 1972). NH is an efficient antifreeze agent, which should allow liquid H_2O-NH-rich subsurface oceans to persist for longer periods of time and at lower temperatures, compared to "pure" liquid H_2O oceans (e.g., J. Leliwa-Kopystyński et al. 2002; H. Hussmann et al. 2006; F. Nimmo & R. Pappalardo 2016). However, NH-rich deposits exposed on Ariel and the other Uranian moons should be efficiently removed over short timescales by magnetospheric charged particle bombardment (~10^6 yr for Ariel's neighboring moon, Miranda; M. H. Moore et al. 2007). In addition to NH-bearing species, ground-based telescope observations and JWST have shown that Ariel's surface is mantled by a large abundance of CO_2 and CO (W. Grundy et al. 2003; W. Grundy et al. 2006; R. J. Cartwright et al. 2015, 2024). Although CO_2 and CO can be actively formed by radiolysis (e.g., S. M. Menten et al. 2024), the spectral signatures of these volatiles on Ariel measured in recent JWST/NIRSpec observations (R. J. Cartwright et al. 2024), and results of recent modeling work (S. M. Menten et al. 2024; T. A. Nordheim et al. 2024, in preparation), indicate that the primary replenishment mechanism for these volatiles are more consistent with exposure by recent geologic activity.

Radiolytic modification of NH-bearing species mixed with H_2O and CO_2 could form other, more refractory constituents that are able to persist over longer timescales, such as carbonate salts that have similar spectral signatures to NH_3 (R. J. Cartwright et al. 2023). Whatever exact combination of components contribute to Ariel's spectral properties in the 2.2 μm wavelength region, it is likely that they have an endogenic origin (R. J. Cartwright et al. 2020) and may have been replenished by cryovolcanic emplacement or exposure of subsurface material by tectonic processes, mass wasting, impact events, or spreading.

If cryovolcanic flows have been emplaced on Ariel's surface, they could have contained NH-bearing species or other efficient antifreeze agents. Furthermore, cryovolcanic processes may have played an important role in resurfacing large regions of Ariel's surface (e.g., D. G. Jankowski & S. W. Squyres 1988; P. M. Schenk 1991; C. B. Beddingfield & R. J. Cartwright 2021). For example, in the region that makes up the intersection of Korrigan and Sylph Chasmata, Agape Crater is partially overprinted by an apparent lobate-shaped feature that could be a cryovolcanic flow deposit. Other nearby features that appear to exhibit morphologies consistent with lobate flow fronts are present in the Young Smooth Materials unit (C. B. Beddingfield & R. J. Cartwright 2021). However, Ariel's lobate features may instead be explained by mass wasting or tectonism (C. B. Beddingfield & R. J. Cartwright 2021).

Interior Properties and Orbital Resonances. Ariel (radius = 579 km) is thought to contain a present-day residual (<30 km thick) interior ocean (J. Castillo-Rogez et al. 2023) and likely experienced intense tidal heating during resonance activity (e.g., M. Ćuk et al. 2020; S. R. Gomes & A. Correia 2024a, 2024b), and some of these resonances drove interior melting (J. Castillo-Rogez et al. 2023). This activity is consistent with high heat fluxes reflected by lithospheric flexure associated with chasmata across Ariel's surface (G. Peterson et al. 2015; C. B. Beddingfield et al. 2022) and by the relaxation state of Yangoor Crater (M. T. Bland et al. 2023). Ariel's estimated past heat fluxes, assuming that Ariel has a pure H_2O ice lithosphere, ranges from 6 to 92 mW m^{-2} and varies spatially and likely temporally. These values are higher than the expected heat fluxes that would have resulted from the hypothesized mean motion resonances (MMRs) shared previously between Ariel and its neighboring satellites (W. C. Tittemore & J. Wisdom 1990; G. Peterson et al. 2015; M. Ćuk et al. 2020; C. B. Beddingfield et al. 2022).

3. Chasma-medial Groove Formation Hypotheses

Three formation models could explain the characteristics of Ariel's chasma floors and medial grooves (Figure 3). In the axial eruption model (B. A. Smith et al. 1986; Figure 3(a)), highly viscous cryovolcanic material welled up along the centers of the chasma floors and flowed laterally to form Ariel's "smooth materials" units. D. G. Jankowski & S. W. Squyres (1988) suggested that perhaps the extruded solid-state cryovolcanic material spread short distances laterally and produced lateral flow fronts that generated troughs along the chasma margins. Retaining the high-standing topography of the hypothesized flow fronts bounding the medial grooves would require viscosities significantly higher than that for pure H_2O ice but would be more in line with combinations of H_2O ice and NH_3 and/or CH_4 ices (D. G. Jankowski & S. W. Squyres 1988; J. Kargel & S. Croft 1989; J. Kargel et al. 1991). As summarized in S. Croft & L. Soderblom (1991), there are issues with this model. For example, the supposed volcanic deposits on the chasma floors are notably uniform and parallel along the chasma lengths, for hundreds of kilometers. This interpretation is inconsistent with cryovolcanic eruptions because uniformity in eruption rates is not expected based on terrestrial fissure studies (e.g., S. Croft & L. Soderblom 1991). For example, during fissure eruptions on Earth, magma flow localization occurs and vent activity is concentrated (e.g., L. Wilson & J. W. Head 1981).

In the lava tube eruption model, the confined-lava tube-fed flows occurred along the chasma floors, forming the medial grooves (S. Croft & L. Soderblom 1991; Figure 3(b)). As the flows moved, snouts formed at the termini, fed by the lava tubes. The lateral margins of the lava cooled, forming steep lateral slopes. As the flows continued, pressures increased in the lava tubes, causing lateral expansion and vertical swelling. These pressures continued until the sides of the flows cooled enough to cease lateral expansion. In some locations, the lateral margins were breached, forming new flows. As the pressures in the lava tubes subsided, the roofs over the tubes sagged and collapsed, producing the medial grooves. S. Croft & L. Soderblom (1991) note that this model accounts for the lobate features at the ends of some flows, the marginal troughs, and the longitudinal uniformity down the chasmata lengths.

In the spreading center model (Figure 3(c)), the centrally located medial grooves (i.e., the axial troughs with raised rims) are spreading centers, analogous to mid-ocean ridges on Earth. In this model, material from Ariel's interior ascended through the grooves, was emplaced on the surface, and formed new crust as the bounding Cratered Plains migrated, creating the newly formed floors of the chasmata (i.e., the young chasma floors). The chasma-medial groove systems originated as rift systems, leading to normal faulting (Time 1). Subsequent spreading created new crust, characterized by lower crater densities, subparallel normal faults, and bowed-up chasma floors (Time 2).

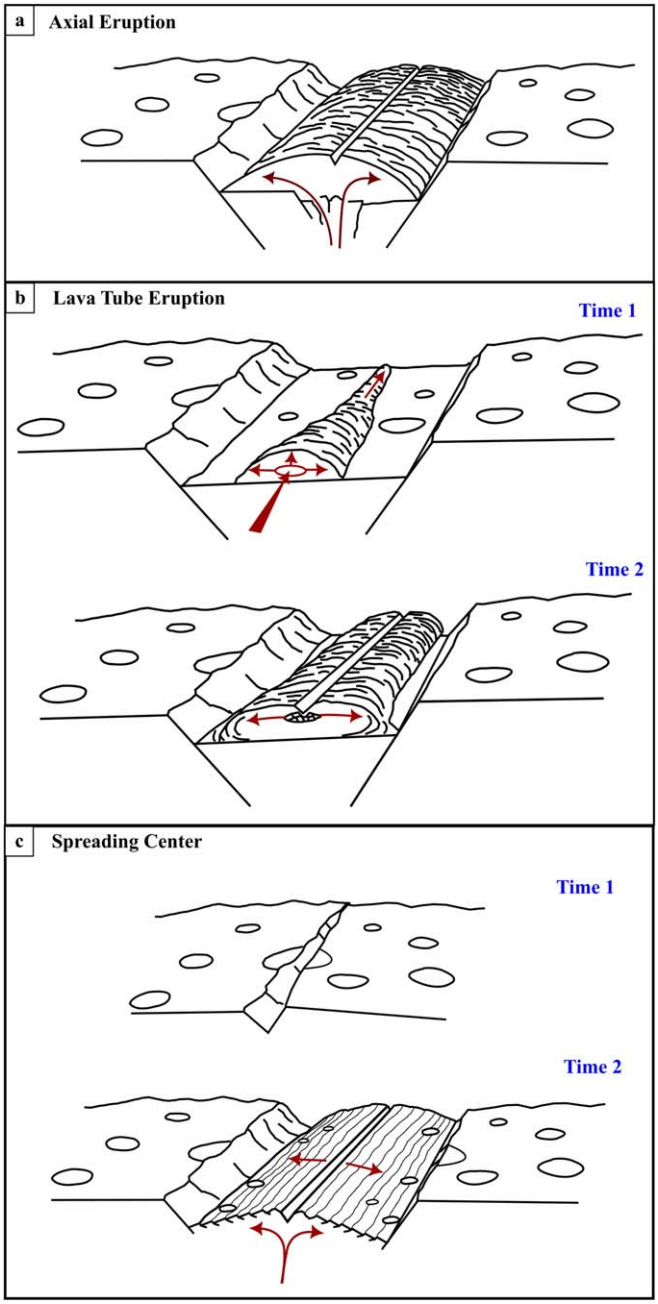

Figure 3. Hypothesized formation models for Ariel's chasma-medial groove systems. (a) In the axial eruption model proposed by B. A. Smith et al. (1986), viscous material welled up along the centers of valley floors and flowed laterally, embaying the bases of adjacent chasmata walls. This figure panel is a digitized version of Figure 11(a) in S. Croft & L. Soderblom (1991). (b) In the lava tube eruption model, proposed by S. Croft & L. Soderblom (1991), confined-lava tube-fed flows took place along the chasma floors (Time 1). As pressures increased in the lava tubes, expansion occurred, and as the pressures subsided, the roofs collapsed, producing medial grooves (Time 2). This figure panel is a digitized version of Figure 11(b) in S. Croft & L. Soderblom (1991). (c) In the spreading center model, Ariel's surface fractures (Time 1), and then warm and buoyant subsurface ice wells up into the gap (Time 2). As the newly resurfaced crust moves away from spreading center, it cools, thickens, and therefore subsides due to a reduction in buoyancy with age, temperature, thickness, and therefore distance from the spreading center.

4. Evidence for Spreading

Here, we show that Ariel's chasma-medial groove systems likely formed via spreading. As summarized in Table 1, while some properties of these systems are consistent with the axial eruption and lava tube eruption models (Section 3), other observations do not support these two models. However, all observed properties of the chasma-medial groove systems support the spreading center interpretation, which includes the following:

Cratered Plains Reconstruction. As shown in Figure 4, the margins of Brownie, Kewpie, Korrigan, Pixie, and Sylph Chasmata closely align when the Intermediate Age Smooth Materials (orange unit in Figure 1), which make up the chasma floors, are removed and the Cratered Plains (green unit in Figure 1) are reconstructed. Two unnamed chasmata and Kra Chasma, which are separated by Kewpie and Pixie Chasmata, respectively, align into a single chasma when the Cratered Plains are reconstructed (yellow bordered ISS image in Figure 1). J. Kargel (1988) found that this offset indicated evidence for large-scale translational displacement.

The three segments of Kra Chasma are the only clearly offset features visible in the available images of Ariel's surface. While there may be other offset geological features, the low resolution of the images makes it challenging to identify them. Some craters could also be offset, but resolution limitations hinder our ability to confirm this. Consequently, our reconstruction relies on removing the young chasma floors, analyzing the offset of the three Kra Chasma segments, and aligning the similarly shaped chasma walls with one another. We can infer from this reconstruction that the two unnamed chasmata once made up Kra Chasma before spreading took place. This interpretation indicates that Kra is an older chasma that formed prior to the spreading events that formed Kewpie and Pixie Chasmata.

Bowed-up Chasma Floors. The central regions of Ariel's chasma floors are raised relative to the marginal troughs, which are present at the bases of the large chasma-bounding normal fault scarps (Profile B–B′ and white arrows in Figure 2(b)). This type of topography is consistent with the expected buoyancy associated with terrain surrounding spreading centers on Earth (e.g., N. H. Sleep & B. R. Rosendahl 1979; S. M. Carbotte & K. C. Macdonald 1994) and Europa (e.g., L. M. Prockter et al. 2002). This topographic signature is due to the spatial variations of the new lithosphere's thickness, temperature, and age adjacent to spreading centers. The youngest, and therefore the thinnest and warmest lithosphere, exists closest to the spreading centers.

As summarized in N. H. Sleep & B. R. Rosendahl (1979), thermal buoyancy causes this warmest lithosphere to uplift to a greater extent, with the greatest amount of uplift being present along the spreading center. This thermal buoyancy causes bowing up of the chasma floors and also creates the low-lying axial margins along where the lithosphere is thicker. In the case of Ariel, these margins are located where the chasma floors meet the Cratered Plains.

Axial Troughs with Raised Rims. The observed topography (Figure 2) associated with much of Ariel's medial grooves is consistent with spreading axis topography on Earth (e.g., H. Menard 1967; N. H. Sleep & B. R. Rosendahl 1979; Y. Chen & W. J. Morgan 1990) and Europa (e.g., R. Sullivan et al. 1998; L. M. Prockter et al. 2002; L. M. Prockter & G. W. Patterson 2009). In terrestrial settings, spreading center topography is a function of the thermal structure at the ridge axis, which is a function of crustal thickness, magma supply, and spreading rate (J. Phipps Morgan & Y. J. Chen 1993). The depths and widths of terrestrial spreading center axial troughs

Table 1
Observations Consistent with Each of the Formation Hypotheses for Ariel's Chasma-medial Groove Systems Illustrated in Figure 3

Observation	Axial Eruption	Lava Tube Eruption	Spreading Center
Bowed-up chasma floors and marginal valleys	✓	✓	✓
Axial troughs with raised rims	✓	✓	✓
Young chasma floors	✓	✓	✓
Chasma margins align when floors removed	×	×	✓
Offset Kra Chasma segments	×	×	✓
Subparallel ridges on chasma floors	×	×	✓

Note. The rationale for whether an observation supports (✓) or refutes (×) a hypothesis is described in Section 3 for the axial and lava tube eruption models and in Section 4 for the spreading center model. Discussions on alignment of chasma margins are shown in Figure 4, and the offset Kra Chasma sections are shown by the white arrows in the yellow-bordered image in Figure 2.

and the heights and spacing of the raised rims decrease with decreasing rates of spreading (H. Menard 1967; Y. Chen & W. J. Morgan 1990).

Subparallel Ridges. Geologic features with topography indicative of tilted normal faults that may be analogous to terrestrial abyssal hills trend subparallel to the medial grooves in some locations (Profile C–C′ in Figure 2).

The spacing and amplitude of these ridges vary across the chasma floors, with the most pronounced features found along the terrain bounding Leprechaun Vallis, where spacing is approximately 20 km, as shown in Profile C–C′ in Figure 2. While subparallel ridges are visible in the digital elevation model (DEM) around this largest and most prominent medial groove, these features are only observable in a few locations surrounding the smaller Sprite Vallis, as seen in Voyager 2 images. In contrast, the smaller medial groove, Unnamed Vallis, shows no detectable ridges in either the DEM or images. This apparent absence of ridge and groove features may be due to image resolution limitations that do not allow their detection in regions bounding smaller valles.

Sets of normal faults form within the terrain bounding spreading centers on Earth and Europa (K. C. Macdonald 1982; R. Sullivan et al. 1998), and their spacing has been found to be a function of spreading rate (e.g., S. M. Carbotte & K. C. Macdonald 1994). Morphological variations along individual spreading centers and from spreading center to spreading center are seen on Europa (e.g., L. M. Prockter et al. 2002) and Earth as well (e.g., J. S.-F. Shih 1979; R. Searle & A. Laughton 1981; K. C. Macdonald 1982, 1986). Similar variations are present along and between Ariel's medial grooves. For example, normal fault scarps bounding spreading centers may be either inward or outward dipping, affecting the locations where steep fault scarps are exposed, thereby affecting topography. Dip directions of normal faults bounding spreading centers are functions of spreading rate (e.g., R. Searle & A. Laughton 1981; S. M. Carbotte & K. C. Macdonald 1994).

Young Chasma Floors. The young age of Ariel's chasma floors relative to the adjacent Cratered Plains is consistent with exposure of new crust from spreading centers. However, the resolutions of Voyager 2 ISS images that cover the chasma floors are too coarse to conduct statistically significant crater counting on these floors. While M. R. Kirchoff et al. (2022), K. Zahnle et al. (2003), and M. E. Borrelli et al. (2025) conducted crater counting studies to estimate surface ages on much of Ariel's surfaces, the floors of these chasmata were excluded from these studies. Therefore, we do not currently have absolute age estimates for Ariel's chasma floors, and comparing crater densities within the chasma floors themselves is difficult.

5. Discussion and Implications

Comparison with Other Bodies. Spreading centers identified on Ariel share many similar properties with those identified on Europa and Earth (Table 2). Evidence for spreading has also been identified on Ganymede based on reconstructions of deformed terrains (A. Pizzi et al. 2017), similar to our reconstruction of Ariel's Cratered Plains. Further studies are required to further investigate the morphologies of Ganymede's spreading centers, specifically to determine whether they exhibit similar morphologies to those observed on Ariel.

The low image resolutions of available images of Ariel may be limiting our identifications of several features including hummocks (small hill-like features) and evidence for subduction-like zones. Although spreading centers on Earth are active, Europa's are likely inactive and represent an extinct style of resurfacing that has since evolved into ubiquitous systems of ridges and chaos terrains, possibly resulting from Europa's lithosphere thickening over time (e.g., L. M. Prockter et al. 2002). In contrast, Ariel's spreading centers cut across its youngest terrains and therefore likely represent the youngest observed geologic feature on this moon, perhaps forming during its most recent period of resurfacing. While absolute modeled age estimates of the chasma floors have not been estimated, results of modeling work by S. R. Gomes & A. Correia (2024a) indicate that Ariel may have been in an MMR with Umbriel 460–920 Myr ago. Therefore, the resurfacing driven by Ariel's increase in eccentricity and resulting tidal heating may have followed this event, occurring more recently.

Additional Medial Grooves. Although medial grooves were only identified in Brownie and Kewpie Chasmata, we hypothesize that additional medial grooves are also present on the floors of Pixie, Korrigan, and Sylph Chasmata but are too small to identify in the ~1 km pixel^{-1} images collected by ISS. The evidence suggesting that these chasmata likely formed through spreading includes the significant offset of Kra Chasma relative to two other unnamed chasmata (yellow-bordered Voyager 2 ISS image in Figure 1; yellow lines in Figure 4), the presence of the bowed-up and young chasma floors (Figure 2(b)), and the closely fitting margins of these chasmata (red boundaries in Figure 4; Table 1).

Future work is needed to investigate crater size frequency distributions of chasma floors, degradation states, and cross-cutting relationships between geologic features proximal to the

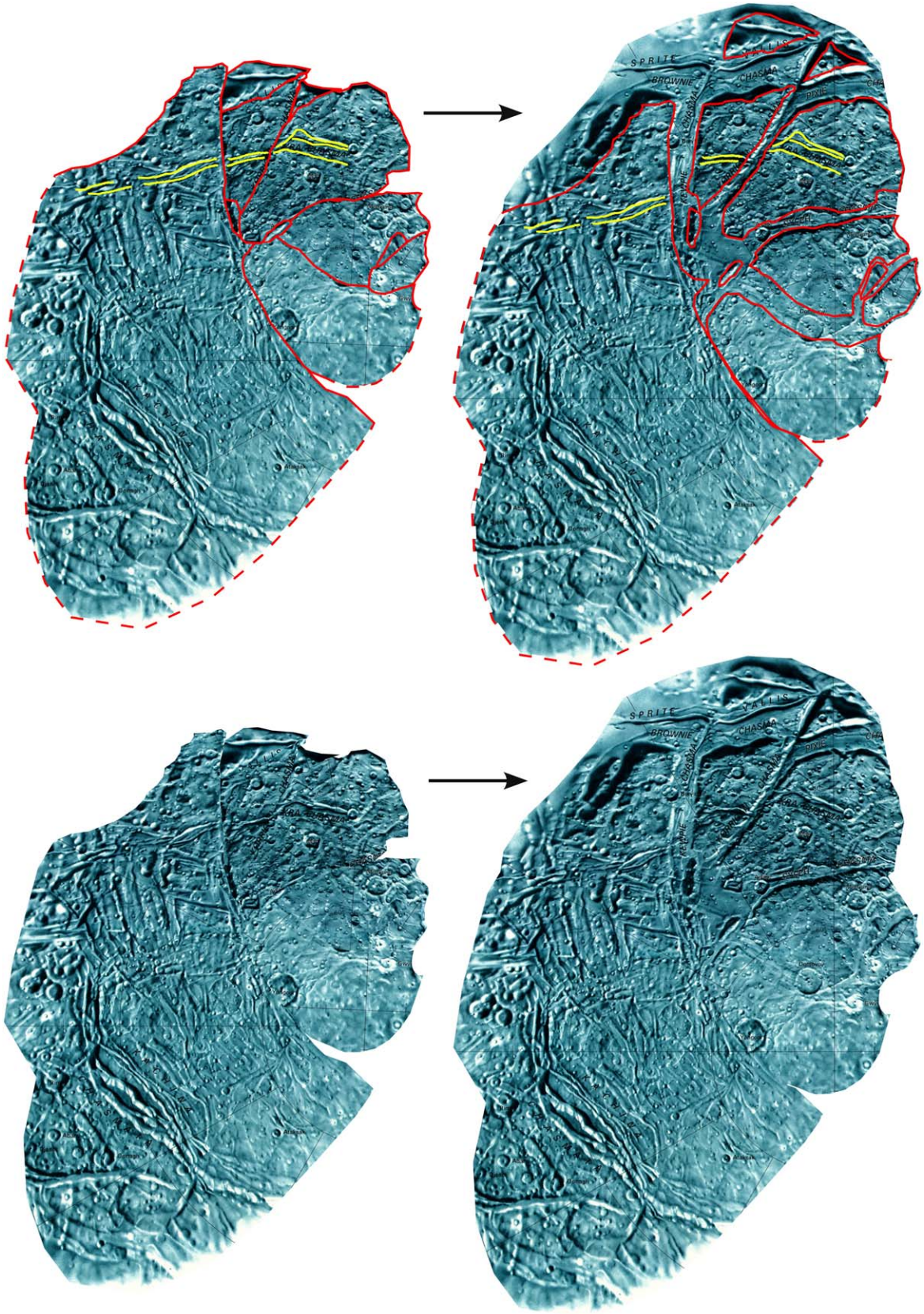

Figure 4. Possible configurations of Ariel's Cratered Plains before (left) and after (right) spreading occurred, creating Ariel's Pixie Group of chasmata, forming the smooth materials units, and offsetting Kra Chasma (yellow). The Cratered Plains boundaries (red) are based on geologic mapping by S. Croft & L. Soderblom (1991) and visual identification of chasma rims in ISS images. These borders are inferred (dashed red) in regions where the boundaries are difficult to identify with certainty due either to low image resolutions or the terrain being close to the terminator. The base Ariel mosaic is from S. Croft & L. Soderblom (1991). Our reconstruction focuses on removing the young chasma floors, examining the offset of the Kra Chasma segments, and aligning the similarly shaped chasma walls. See Figure 1 for geologic feature labels.

Table 2
Comparison of Spreading Center Properties Identified on Ariel, Earth, and Europa

Spreading Center Properties	Ariel	Earth	Europa
Younger bounding terrains	✓	✓	✓
Central axial troughs	✓	✓	✓
Ridges and grooves	✓	✓	✓
Regional bowed-up terrain	✓	✓	✓
Offset geologic features	✓	✓	✓
Hummocks	×	✓	✓
Subduction-like zones	×	✓	×

medial grooves to discern the relative ages of the individual chasmata and to further test for additional medial grooves.

Convection. Tidal heating driven by past orbital resonance events between Ariel and Umbriel would have increased Ariel's eccentricity (M. Ćuk et al. 2020; S. R. Gomes & A. Correia 2024a, 2024b). This activity may have, in turn, driven interior convection, lithospheric fracturing, and subsequent spreading activity. This interpretation is consistent with large spatial variations in past heat fluxes identified across Ariel's imaged surface associated with the chasmata (G. Peterson et al. 2015; C. B. Beddingfield et al. 2022). The spatial heat flux variations may reflect regional heat concentration due to internal convection processes, in particular in the chasma-medial groove system region. Areas associated with higher heat fluxes might overlie the center of upwelling convection cells, while locations associated with less elevated heat fluxes might represent the cell's downwelling margins (see Figure 9 in C. B. Beddingfield et al. 2022).

Subduction. Due to the large amount of extension associated with Ariel's multiple spreading centers, accommodating contractional terrain, such as subduction-like zones, may also be present on Ariel. However, the contractional geologic features that we would expect at subduction-like zones have not been identified in Voyager 2 images of Ariel. Perhaps these features are present in the unimaged terrains or are not identifiable in available Voyager 2 ISS images. We expect these contractional features to trend subparallel to the orientations of the observed spreading centers. These features might be located within the Cratered Plains (green unit in Figure 1) or north of the equator on the Uranus-facing hemisphere, beyond Sprite and Leprechaun Valles.

Conduits to the Interior. The presence of medial grooves at locations where new surface material has formed on chasma floors indicates that these grooves are primary zones of weakness in Ariel's lithosphere. Given the compelling evidence that these medial grooves have transported interior material to the surface to form new crust, they are more likely sources of any internally derived CO and CO_2, in contrast to other fractures, which show no evidence of facilitating the movement of subsurface material. While Ariel's other fractures may still function as secondary conduits, their contribution is likely minimal in comparison. Additional medial grooves associated with spreading may be present in areas of Ariel that have not been imaged, or they could be below the resolution of the available Voyager 2 ISS images in the regions that have been imaged. If present, these additional grooves may also act as significant conduits to the interior.

On Earth, discrete volcanic eruptions occur along spreading centers, often within the axial troughs (e.g., S. A. Soule 2015). As summarized in S. A. Soule (2015), the character and frequency of terrestrial spreading center volcanic eruptions are functions of spreading rate. On Ariel, eruptions associated with spreading might have also occurred. If these eruptions took place, perhaps they exhibited a similar style of volcanism to Enceladus's Tiger Stripe plumes (e.g., J. R. Spencer et al. 2009), where erupted cryovolcanic material degasses and sublimates more rapidly than cryolava can be emplaced on the surface. However, higher-resolution images are needed to test this hypothesis and to fully access any evidence for plume deposits bounding spreading centers.

On Ariel, the emerging spectroscopic picture suggests that CO_2 and CO ice, NH-bearing species, and other volatiles may originate in its interior, as opposed to primarily resulting from charged particle bombardment (R. J. Cartwright et al. 2024). Ariel's medial grooves might represent the pathways utilized by CO_2 and other carbon oxides to reach its surface. Perhaps the medial grooves are also the source of neutrals to Uranus's magnetosphere and ultimately the energetic ions observed between the orbits of Miranda and Ariel (I. J. Cohen et al. 2023). Recent results by T. A. Nordheim et al. (2024, in preparation) further supports this hypothesis, as they conclude that the distribution of CO_2 observed on Ariel's surface is not consistent with a radiolytic origin due to magnetospheric bombardment and may instead be from an endogenic source.

6. Future Observations with a Uranus Orbiter

Ariel's medial grooves represent some of the youngest surface features and could probe its internal chemistry, making them important targets of study for the Uranus Orbiter and Probe (UOP) mission. By investigating these medial grooves with instruments on board UOP, important science questions can be addressed. Investigating Ariel's medial grooves using topography derived from stereophotoclinometry will be critical. Europan spreading centers were analyzed in detail using multiple images of identified bands with resolutions ranging from 14 to 220 m pixel^{-1} from Galileo's Solid State Imager (SSI; e.g., L. M. Prockter et al. 2002). If some spreading centers on Ariel exhibit similar scales to those on Europa, with spreading axes well below 1 km in width, then stereo image pairs with resolutions of at least 20 m pixel^{-1} are needed to fully characterize these features.

High-resolution images from a camera on board UOP will allow for investigations into spreading rates and therefore constraints on how long Ariel has been geologically active. Predicting Ariel's spreading rates in this study is challenging due to the many variables involved in generating the observed topography at spreading centers, such as lithospheric thickness, magma supply, and other lithospheric properties. Additionally, the limited resolution of available images makes it difficult to even qualitatively assess the spreading rates. Future studies could use modeling and Voyager 2 images to constrain spreading rates that can be tested when UOP arrives though this is beyond the scope of the current work.

Morphological analyses of medial grooves and bounding terrains in high-resolution images will shed light on the rheological, thermal, and structural properties of the interior. Investigating the spacing and heights of the chasma floor ridges will allow us to estimate the elastic thicknesses and interior temperature profiles, which are important indicators of habitability. Investigating crater size frequency distributions on chasma floors will allow for absolute age estimates of some

of Ariel's youngest known surfaces, providing important constraints on the timing of geologic activity.

Obtaining compositional information along the medial grooves at 100 m pixel^{-1} with a near-infrared imaging spectrometer would allow us to determine whether CO_2 and CO, and possibly carbonates and NH-bearing species, are spatially correlated with the medial grooves. A correlation would be consistent with an endogenic origin for these species, thereby strengthening Ariel's potential ocean world status. Additionally, the thermal properties of these features and other regions of Ariel's surface could be assessed from data collected with a thermal-infrared imager, providing key clues on whether these features were recently active. If outgassing from plume activity is occurring along the medial grooves, then ultraviolet imaging would allow us to detect and measure this process and would reveal critical insight into Ariel's internal composition.

7. Conclusions

Our results indicate that medial grooves in large chasmata on Ariel are spreading centers, resulting from the exposure of subsurface material, creating new crust. Thus, these features are likely geologic conduits to Ariel's interior and could be the primary source of CO_2, CO, and other volatiles detected on its surface. Voyager 2 images directly revealed medial grooves in Brownie and Kewpie Chasmata, and our results indicate that these features are likely also present in Korrigan, Pixie, and Sylph Chasmata although they are not directly observed. However, medial grooves are inferred in these locations based on the presence of bowed-up floors and closely fitting chasma margins. The medial grooves are some of the youngest geologic features observed on Ariel, and close flybys of these features by a future Uranus orbiter are imperative to gain insight into recent geologic events and the geologic and geochemical properties of this candidate ocean world.

Acknowledgments

This publication was supported by investments of internal development funds from the Johns Hopkins University Applied Physics Laboratory.

We would like to thank the anonymous reviewers for insightful and constructive reviews of this paper.

ORCID iDs

Chloe B. Beddingfield https://orcid.org/0000-0001-5048-6254
Richard J. Cartwright https://orcid.org/0000-0002-6886-6009
Lauren M. Jozwiak https://orcid.org/0000-0001-7946-5633
Tom A. Nordheim https://orcid.org/0000-0001-5888-4636
G. Wes Patterson https://orcid.org/0000-0003-4787-3899

References

Beddingfield, C. B., & Cartwright, R. J. 2021, A Lobate Feature Adjacent to a Double Ridge on Ariel: Formed by Cryovolcanism or Mass Wasting?, Icar, 367, 114583
Beddingfield, C. B., Cartwright, R. J., Leonard, E. J., Nordheim, T. N., & Scipioni, F. 2022, Ariel's Elastic Thicknesses and Heat Fluxes, PSJ, 3, 106
Bland, M. T., Beddingfield, C. B., Nordheim, T. A., Patthoff, D. A., & Vance, S. D. 2023, Constraints on the Composition and Thermal Structure of Ariel's Icy Crust as Inferred from its Largest Observed Impact Crater, Icar, 395, 115452
Borrelli, M. E., Bierson, C. J., & O'Rourke, J. G. 2025, Simple-to-complex Crater Transition for the Uranian Satellites Ariel and Miranda, JGRE, 130, e2024JE008507
Carbotte, S. M., & Macdonald, K. C. 1994, The Axial Topographic High at Intermediate and Fast Spreading Ridges, E&PSL, 128, 85
Cartwright, R. J., Beddingfield, C., Nordheim, T., et al. 2020, Evidence for Ammonia-bearing Species on the Uranian Satellite Ariel Supports Recent Geologic Activity, ApJL, 898, L22
Cartwright, R. J., DeColibus, R. A., Castillo-Rogez, J. C., et al. 2023, Evidence for Nitrogen-bearing Species on Umbriel: Sourced from a Subsurface Ocean, Undifferentiated Crust, or Impactors?, PSJ, 4, 42
Cartwright, R. J., Emery, J. P., Pinilla-Alonso, N., et al. 2018, Red Material on the Large Moons of Uranus: Dust from the Irregular Satellites?, Icar, 314, 210
Cartwright, R. J., Emery, J. P., Rivkin, A. S., Trilling, D. E., & Pinilla-Alonso, N. 2015, Distribution of CO_2 Ice on the Large Moons of Uranus and Evidence for Compositional Stratification of their Near-surfaces, Icar, 257, 428
Cartwright, R. J., Holler, B. J., Grundy, W. M., et al. 2024, JWST Reveals CO Ice, Concentrated CO_2 Deposits, and Evidence for Carbonates Potentially Sourced from Ariels Interior, ApJL, 970, L29
Castillo-Rogez, J., Weiss, B., Beddingfield, C., et al. 2023, Compositions and Interior Structures of the Large Moons of Uranus and Implications for Future Spacecraft Observations, JGRE, 128, e2022JE007432
Chen, Y., & Morgan, W. J. 1990, A Nonlinear Rheology Model for Mid-ocean Ridge Axis Topography, JGR, 95, 17583
Cohen, I. J., Turner, D. L., Kollmann, P., et al. 2023, A Localized and Surprising Source of Energetic Ions in the Uranian Magnetosphere Between Miranda and Ariel, GeoRL, 50, e2022GL101998
Croft, S., & Soderblom, L. 1991, Geology of the Uranian Satellites, Uranus (Tucson, AZ: Univ. Arizona Press), 561
Ćuk, M., Moutamid, M. E., & Tiscareno, M. S. 2020, Dynamical History of the Uranian System, PSJ, 1, 22
Gomes, S. R., & Correia, A. 2024a, Dynamical Evolution of the Uranian Satellite System I. From the 5/3 Ariel-Umbriel Mean Motion Resonance to the Present, Icar, 424, 116282
Gomes, S. R., & Correia, A. 2024b, Dynamical Evolution of the Uranian Satellite System II. Crossing of the 5/3 Ariel-Umbriel Mean Motion Resonance, Icar, 424, 116254
Grundy, W., Young, L., Spencer, J., et al. 2006, Distributions of H_2O and CO_2 Ices on Ariel, Umbriel, Titania, and Oberon from IRTF/SpeX Observations, Icar, 184, 543
Grundy, W., Young, L., & Young, E. 2003, Discovery of CO_2 Ice and Leading–Trailing Spectral Asymmetry on the Uranian Satellite Ariel, Icar, 162, 222
Hanel, R., Conrath, B., Flasar, F., et al. 1986, Infrared Observations of the Uranian System, Sci, 233, 70
Hussmann, H., Sohl, F., & Spohn, T. 2006, Subsurface Oceans and Deep Interiors of Medium-sized Outer Planet Satellites and Large Trans-neptunian Objects, Icar, 185, 258
Jankowski, D. G., & Squyres, S. W. 1988, Solid-state Ice Volcanism on the Satellites of Uranus, Sci, 241, 1322
Kargel, J. 1988, Liquidus Phase Relations and Liquid Properties in the System H2O-NH3-CO2-H2CO, LPSC, 19, 583
Kargel, J., & Croft, S. 1989, Rheological Extremes of Cryogenic Liquids on Icy Satellites, LPSC, 698, 47
Kargel, J., Croft, S., Lunine, J., & Lewis, J. 1991, Rheological Properties of Ammonia-water Liquids and Crystal-liquid Slurries: Planetological Applications, Icar, 89, 93
Kirchoff, M. R., Dones, L., Singer, K., & Schenk, P. 2022, Crater Distributions of Uranus's Mid-sized Satellites and Implications for Outer Solar System Bombardment, PSJ, 3, 42
Leliwa-Kopystyński, J., Maruyama, M., & Nakajima, T. 2002, The Water–Ammonia Phase Diagram up to 300 MPa: Application to Icy Satellites, Icar, 159, 518
Lewis, J. S. 1972, Metal/Silicate Fractionation in the Solar System, E&PSL, 15, 286
Macdonald, K. C. 1982, Mid-ocean Ridges: Fine Scale Tectonic, Volcanic and Hydrothermal Processes within the Plate Boundary Zone, AREPS, 10, 155
Macdonald, K. C. 1986, The Crest of the Mid-Atlantic Ridge: Models for Crustal Generation Processes and Tectonics, The Western North Atlantic Region (McLean, VA: Geology of North America), 51
Menard, H. 1967, Sea Floor Spreading, Topography, and the Second Layer, Sci, 157, 923
Menten, S. M., Sori, M. M., Bramson, A. M., Nordheim, T. A., & Cartwright, R. J. 2024, Volatile Transport on Ariel and Implications for the Origin and Distribution of Carbon Dioxide on Uranian Moons, JGRE, 129, e2024JE008376
Moore, M. H., Ferrante, R., Hudson, R., & Stone, J. 2007, Ammonia–Water Ice Laboratory Studies Relevant to Outer Solar System Surfaces, Icar, 190, 260

Nimmo, F., & Pappalardo, R. 2016, Ocean Worlds in the Outer Solar System, JGRE, 121, 1378
Peterson, G., Nimmo, F., & Schenk, P. 2015, Elastic Thickness and Heat Flux Estimates for the Uranian Satellite Ariel, Icar, 250, 116
Phipps Morgan, J., & Chen, Y. J. 1993, Dependence of Ridge-axis Morphology on Magma Supply and Spreading Rate, Natur, 364, 706
Pizzi, A., Di Domenica, A., Komatsu, G., et al. 2017, Spreading versus Rifting as Modes of Extensional Tectonics on the Globally Expanded Ganymede, Icar, 288, 148
Plescia, J. 1987, Geological Terrains and Crater Frequencies on Ariel, Natur, 327, 201
Prockter, L. M., Head, J. W., III, Pappalardo, R. T., et al. 2002, Morphology of Europan Bands at High Resolution: A Mid-ocean Ridge-type Rift Mechanism, JGRE, 107, 5028
Prockter, L. M., & Patterson, G. W. 2009, Morphology and Evolution of Europa's Ridges and Bands, in Europa, ed. R. T. Pappalardo, W. B. McKinnon, & K. K. Khurana (Tucson, AZ: Univ. Arizona Press), 237
Rothery, D. 1990, Collapsed "Lava" Tubes on Ariel?, LPSC, 21, 1039
Schenk, P. M. 1991, Fluid Volcanism on Miranda and Ariel: Flow Morphology and Composition, JGR, 96, 1887
Schenk, P. M., & Moore, J. M. 2020, Topography and Geology of Uranian Mid-sized Icy Satellites in Comparison with Saturnian and Plutonian Satellites, RSPTA, 378, 20200102
Searle, R., & Laughton, A. 1981, Fine-scale Sonar Study of Tectonics and Volcanism on the Reykjanes Ridge, AcOc, 26, 5, https://archimer.ifremer.fr/doc/00245/35665/
Shih, J. S.-F. 1979, PhD Thesis, Massachusetts Institute of Technology
Sleep, N. H., & Rosendahl, B. R. 1979, Topography and Tectonics of Mid-oceanic Ridge Axes, JGR, 84, 6831
Smith, B. A., Soderblom, L., Beebe, R., et al. 1986, Voyager 2 in the Uranian System: Imaging Science Results, Sci, 233, 43
Sori, M. M., Bapst, J., Bramson, A. M., Byrne, S., & Landis, M. E. 2017, A Wunda-full World? Carbon Dioxide Ice Deposits on Umbriel and Other Uranian Moons, Icar, 290, 1
Soule, S. A. 2015, The Encyclopedia of Volcanoes (Amsterdam: Elsevier), 395
Spencer, J. R., Barr, A. C., Esposito, L. W., et al. 2009, Enceladus: An Active Cryovolcanic Satellite, Saturn from Cassini-Huygens (Berlin: Springer), 683
Sullivan, R., Greeley, R., Homan, K., et al. 1998, Episodic Plate Separation and Fracture Infill on the Surface of Europa, Natur, 391, 371
Team, V. I. S. 1988, Voyager 2 ISS Science Team Data Set: VG2-S-ISS-2-EDR-V1.0, PDS Cartography and Imaging (IMG) Node, NASA Planetary Data System, doi:10.17189/1520365
Thomas, P. 1988, Radii, Shapes, and Topography of the Satellites of Uranus from Limb Coordinates, Icar, 73, 427
Tittemore, W. C., & Wisdom, J. 1990, Tidal Evolution of the Uranian Satellites: III. Evolution through the Miranda-Umbriel 3:1, Miranda-Ariel 5:3, and Ariel-Umbriel 2:1 Mean–Motion Commensurabilities, Icar, 85, 394
Wilson, L., & Head, J. W., III 1981, Ascent and Eruption of Basaltic Magma on the Earth and Moon, JGR, 86, 2971
Zahnle, K., Schenk, P., Levison, H., & Dones, L. 2003, Cratering Rates in the Outer Solar System, Icar, 163, 263